JOURNAL OF MATERIALS SCIENCE **36** (2001) 3129–3135

Deformation mechanisms in cellulose fibres, paper and wood

S. J. EICHHORN, J. SIRICHAISIT, R. J. YOUNG*
Materials Science Centre, UMIST/University of Manchester,
Grosvenor Street, Manchester, M1 7HS, UK
E-mail: robert.young@umist.ac.uk

The use of Raman spectroscopy in probing the deformation mechanisms of cellulose fibres (regenerated and natural), and two natural cellulose composite systems (wood and paper) is described. It is shown that during tensile deformation the 1095 cm^{-1} Raman band, corresponding to the stretching of the cellulose ring structure, shifts towards a lower wavenumber due to molecular deformation. By analysing a number of fibres with different microstructures this shift is shown to be invaluable in understanding the micromechanisms of deformation in these materials. Moreover, the rate of Raman band shift is shown to be invariant with stress for all fibre types, consistent with a fibre microstructure based on a modified series aggregate model. In the composite systems, such as wood and paper, it is shown that the stress-induced Raman band shift in the cellulose gives an important insight into their local deformation micromechanics.

1. Introduction

Raman spectroscopy is an invaluable method for evaluating changes that occur in a fibre structure subjected to stress and strain. It allows the molecular deformation mechanisms of the polymeric chains to be examined through the large stress-induced Raman band shifts that can occur during deformation. It has been applied successfully to study deformation processes for a wide variety of polymeric fibres [1]. It has been found that the magnitude of the wavenumber shift of the Raman-active bands in fibres subjected to stress or strain depends on both the chemical structure of the polymer molecules, and the morphology and microstructure of the fibres. In particular, the band shift rate per unit stress for the 1610 cm^{-1} Raman band for all aromatic main-chain polymeric fibres has been found to be −4 cm^{-1}/GPa. This has been interpreted as a demonstration that the molecules in such fibres are subjected to a uniform stress deformation [1].

The class of polymers based on cellulose include natural cellulose, regenerated cellulose, and chemical derivatives of cellulose such as cellulose acetate and cellulose nitrate. Plants are made from natural cellulose and this can be chemically modified in a regeneration process to produce fibres with very different mechanical properties. The crystal structure of natural cellulose is known as cellulose I, and that of regenerated cellulose as cellulose II. Cellulose I is thought to have a crystal structure wherein the chains in the unit cell are in a parallel conformation [2], and in cellulose II they are thought to be in anti-parallel conformation [3]. The deformation of natural [4] and regenerated cellulose fibres [5] has previously been investigated using Raman spectroscopy. In this work, a comparison between the deformation of regenerated and natural cellulose fibres will be focussed upon.

Man-made, and natural composite systems of cellulose are in widespread use as materials in the industrial world; paper and wood being two examples. Wood can be considered to be a highly complex composite material consisting of fibres, composed mainly of cellulose, embedded in a matrix of lignin and hemicellulose [6]. The fibres themselves are composite structures consisting of several layers (Primary, S_1, S_2 and S_3), of which the middle layer (S_2) is thought to dominate mechanically [6]. One previous investigation has measured micro-mechanical strains within woody materials, using Digital Image Correlation (DIC) to assess the local strain around defects in wood pulp fibres [7]. The micromechanics of small sections of wood have also been studied, and models applied to understand the evolution of the Young's modulus during axial straining [8]. However, little or no work exists on following local strain within wood samples during deformation, and this work focuses on this area.

Paper cannot strictly be classed as a composite material as it is a fibrous network which does not reinforce a matrix but relies on inter-fibre bonding and fibre stiffness for its strength. A number of models for its deformation have been proposed [9–11] and each relies on assumptions about local fibre deformation within the sheet to describe its non-linear stress-strain curve. This study reports the measurement of local fibre deformation in pilot-machine made paper using Raman spectroscopy.

---

* Author to whom all correspondence should be addressed.

0022–2461 © *2001 Kluwer Academic Publishers*

2. Experimental procedure

2.1. Materials

Six different regenerated cellulose fibres were investigated. Fibres (CA-CD) were produced by the viscose process, CE by an alternative solution spinning process and CF produced by the NMMO (N-methylmorpholine N-oxide) process. Fibres CA-CE were provided by Akzo Nobel and CF by Courtaulds (now merged with Akzo Nobel as ACORDIS). The trade names of CA, CB, CC, CD, CE, and CF are Cordenka-EHM, Cordenka-1840, Enka Viscose, Cordenka-700, Alternative Cellulose and Lyocell respectively.

Steam exploded flax and field retted hemp fibres were also examined. The steam exploded flax was produced as hackling tow and processed by FH, Reutlingen, Denmark and the hemp was provided by the British Fibre Federation, UK. Single fibres (5 mm in length) of the natural cellulose fibres were extracted from larger bundles by placing in hydrogen peroxide for 48 hrs. This had the effect of bleaching the fibre, which reduced fluorescence under the Raman laser, and also assisted in releasing the fibres from the stems.

Sections of *Pinus radiata* wood were also investigated. The *Pinus radiata* samples used had a microfibril angle of 13°, measured using small angle x-ray scattering (SAXS) as described elsewhere [12]. The cotton paper studied had been produced on a pilot plant machine in the Department of Paper Science, UMIST.

2.2. Single-fibre deformation

Single fibres were tested using an Instron 1121 universal testing machine following recommendations given in ASTM D3379-75, at $23 \pm 10\,^{\circ}$C and $50 \pm 5\%$ relative humidity. The regenerated cellulose fibres (50 mm gauge length) were tested at a strain rate of 0.166 %/s, and the natural fibres at 0.333 %/s, and a full-scale load of 1N was used. The diameters of the fibres were measured using a calibrated Phillips FEG-SEM with an exciting voltage of 2 keV and these values are reported in Table I. From these values, and assuming a circular cross section, the cross-sectional areas were calculated and thus the load could be converted to stress. Examples of SEM micrographs obtained for the fibres are shown in Fig. 1. For statistical reasons 30 natural fibres were tested, whereas only 20 regenerated fibres were required for the same significance.

TABLE I Mechanical properties of cellulose fibres, where d_f—fibre diameter (30 measurements), E—Young's Modulus, σ_f^*—breaking stress and ε_f^*—breaking strain. Number of mechanical tests (CA-CF—20, Flax and Hemp—30)

Fibre	Sample	d_f (μm)	E (GPa)	σ_f^* (GPa)	ε_f^* (%)
CA	Cordenka EHM	9.4 ± 0.2	32.2 ± 2.2	0.71 ± 0.12	3.9 ± 0.7
CB	Cordenka 1840	12.9 ± 0.3	16.9 ± 1.5	0.66 ± 0.08	12.7 ± 1.4
CC	Enka Viscose	18.0 ± 0.7	9.4 ± 0.5	0.22 ± 0.05	17.2 ± 1.3
CD	Cordenka 700	13.1 ± 1.3	20.0 ± 6.1	0.66 ± 0.01	10.7 ± 0.4
CE	Alternative cellulose	15.6 ± 1.1	30.6 ± 0.1	1.01 ± 0.07	4.9 ± 0.3
CF	Lyocell	12.3 ± 0.9	15.2 ± 2.9	0.54 ± 0.01	7.0 ± 0.3
Flax	Steam Exploded	17.1 ± 2.9	43.5 ± 4.2	0.27 ± 0.03	5.5 ± 0.4
Hemp	Field Retted	31.2 ± 4.9	19.1 ± 4.3	0.27 ± 0.04	0.8 ± 0.1

2.3. Raman spectroscopy

A Renishaw 1000 Raman Imaging Microscope was used to record the spectra of fibre monofilaments. A low power 25 mW He-Ne laser (633 nm) was employed with an intensity of 1 mW when focussed on the monofilament. An infra-red laser (780 nm) was used for the wood and paper samples to overcome fluorescence. The low power laser spot diameter was about 2 μm. A highly-sensitive Peltier-cooled charge couple device (linked to a PC with Renishaw software) was used to record spectra. The spectra were curve fitted using a mixed Lorentzian-Gaussian distribution function to determine the peak positions based on a mathematical algorithm [13].

2.4. Raman deformation studies

Cellulose fibres with a gauge length of 50 mm for CA-CF and 5 mm for flax and hemp were fixed using cyanoacrylate adhesive on a tensile deformation rig that fitted directly onto the stage of the microscope. The fibre axis was aligned parallel to the incident polarised laser beam to within ±5°. For the Raman deformation analysis, each straining increment required 150 s, which included 120 s for exposure and 30 s for the focussing. The fibre stress was recorded using a purpose-built rig, housing a load cell with a full-scale load of 2N and Raman spectra were obtained during deformation.

The wood samples were sectioned into small slivers, which were then secured onto PMMA beams with adhesive. A strain gauge was attached to the beams close to where Raman spectra were obtained. Samples were then deformed using a 4-point-bending rig, and the strain was recorded on a digital multi-meter. An exposure time of 5 minutes, with 5 accumulations, was used at each strain level. The paper samples were cut from a sheet using a razor blade to dimensions of 15×5 mm and glued to the straining rig. At each strain level the samples were exposed with the laser for 120 s.

3. Results and discussion

3.1. Cellulose fibres deformation

The stress-strain curves for Fibres CA-CF are shown in Fig. 2, along with those for flax and hemp fibres. The regenerated cellulose fibres exhibit non-linear stress-strain curves. Each regenerated fibre exhibits characteristic behaviour with an initially linear section, a knee at the yield point and an approximately linear increase after yielding. It is noted, however, that the higher modulus fibres show more strain hardening. The flax and hemp fibres, however, show near linear elastic behaviour with some strain hardening apparent in the hemp fibre samples. The mechanical properties of the fibre samples are listed in Table I.

Typical Raman spectra for a regenerated and a natural cellulose fibre are shown in Fig. 3. For regenerated cellulose fibres there are peaks located at 1095 cm^{-1} and 895 cm^{-1} corresponding to the cellulose C–O ring stretching, and mixed modes (C–C–C, C–H–O) including angle bending respectively [14]. However, in

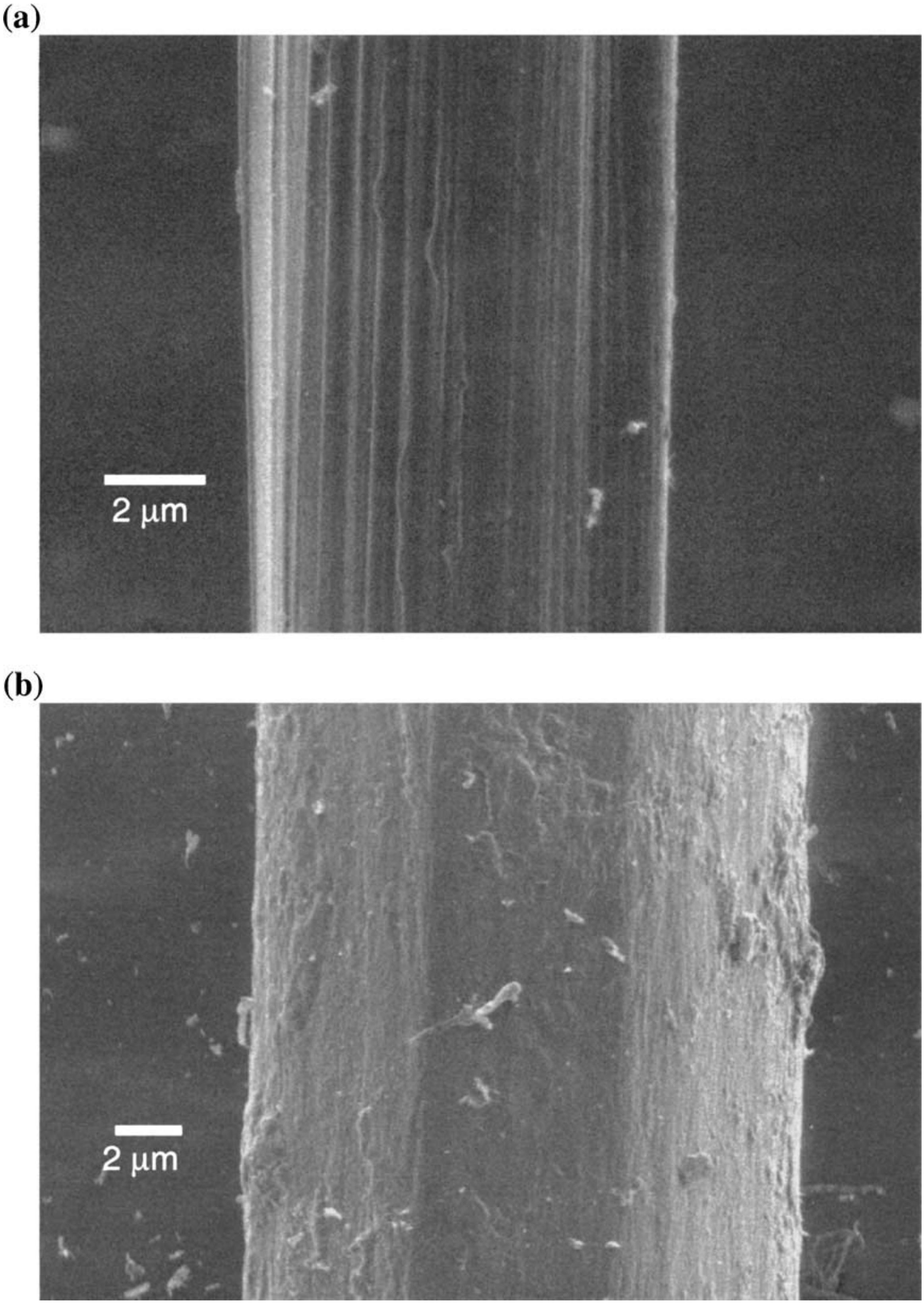

Figure 1 SEM micrographs of (a) CA fibres and (b) steam exploded flax fibres.

natural cellulose it was found that no peak occurred at the 895 cm^{-1} position. It has been reported that the Raman peak located at 895 cm^{-1} is more intense in highly-crystalline cellulose II fibres, compared to *Valonia ventricosa* (cellulose I) [15]. For this reason, only the shift of the 1095 cm^{-1} peak was used for comparison between samples. This peak is also clearly a composite peak, and hence to locate its precise position, the region from 1080–1120 cm^{-1} was fitted using 4 Lorentzian/Gaussian peaks to account for the shoulder peaks located at 1145 cm^{-1} and 1120 cm^{-1}.

Fig. 4 shows examples of shifts for the 1095 cm^{-1} Raman peak for the high modulus CE fibre and for flax. This shift is thought to be due to deformation of

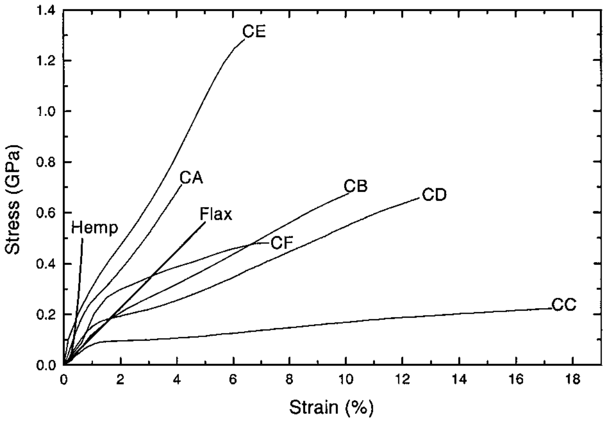

Figure 2 Typical stress strain curves of CA (Cordenka EHM), CB (Cordenka 1840), CC (Enka Viscose), CD (Cordenka 700), CE (Alternative cellulose) and CF (Lyocell) regenerated cellulose fibres and Steam Exploded Flax and Field Retted Hemp fibres. These curves are examples of the typical form of the stress-strain curves, not averages.

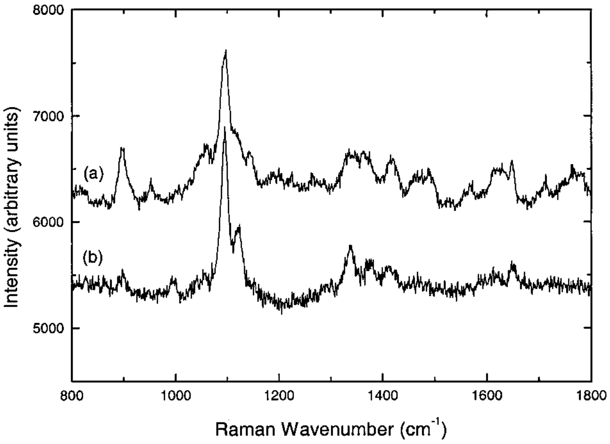

Figure 3 Raman spectra of (a) regenerated cellulose, CA (b) natural cellulose, flax.

the structural molecular backbone of cellulose as has been found with other polymer fibres [16].

The 1095 cm^{-1} peak was found to shift approximately linearly with strain for all fibres towards a lower wavenumber with tensile strain, as can be seen from Fig. 5a. The strain sensitivities of the Raman bands for the different fibres (mean of at least 3 sets of measurements for the regenerated and 10 for the natural cellulose) are summarised in Table II. Despite the very different mechanical properties of the fibres, the fact that the regeneration process is different for each fibre type, and that different cellulose crystal structures (I & II) have been investigated, the stress sensitivity of the Raman band is found to be invariant (Table II). This is best illustrated with reference to Fig. 5b where the linear fits for the Raman band shifts against stress lie on the same line. Because of this stress invariance, which has been found for some other rigid-chain polymer fibres such as aramids [16], it indicates that the shift is controlled by stress. Also, based on this argument it is proposed that the deformation could be analysed using a modified series structural model as has been reported previously [5].

TABLE II Raman band shift sensitivities for cellulose fibres, where $d\Delta\nu/d\varepsilon$ and $d\Delta\nu/d\sigma$ are the rates of Raman shift with strain and stress respectively. Number tested (5 for CA-CF and 10 for flax and hemp)

Fibre	$d\Delta\nu/d\varepsilon$ (cm^{-1}/%)	$d\Delta\nu/d\sigma$ (cm^{-1}/GPa)
CA	-0.88 ± 0.05	-4.34 ± 0.30
CB	-0.22 ± 0.03	-3.94 ± 0.66
CC	-0.06 ± 0.02	-4.89 ± 2.09
CD	-0.29 ± 0.04	-4.17 ± 0.21
CE	-0.74 ± 0.04	-3.53 ± 0.25
CF	-0.18 ± 0.03	-4.13 ± 0.77
Flax	-1.22 ± 0.18	-3.38 ± 0.43
Hemp	-1.29 ± 0.10	-4.07 ± 0.55

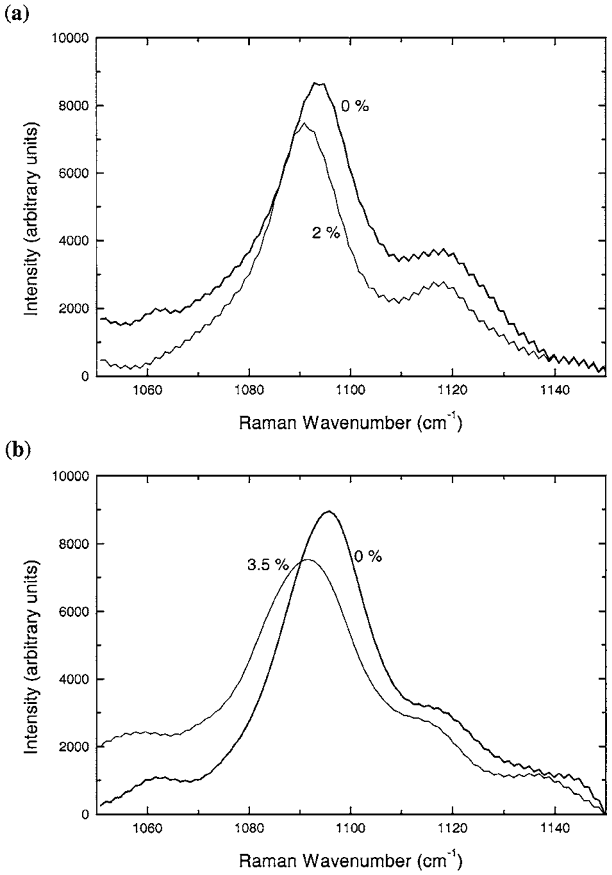

Figure 4 Strain induced Raman band shifts in the smoothed spectra for the 1095 cm^{-1} peaks of (a) CE and (b) flax fibres.

The sensitivity of the position of the Raman band to strain for the cellulose fibres was found to be proportional to the fibre modulus, E, as illustrated in Fig. 6. This is also predicted by the series model and similar behaviour is also found for the 1610 cm^{-1} Raman band in aromatic polymer fibres [1]. The secant modulus was used in Fig. 6 due to the fact that the fibres exhibit different levels of strain hardening beyond the yield point and hence the Young's modulus has been found to not to give such a good correlation [5]. Better correlation is found with the secant modulus because some fibres, such as fibre CC, have more significantly different deformation beyond the yield point which is not taken into account by using the initial modulus and therefore this parameter is more indicative of overall behaviour. If the shift of the Raman band position, $\Delta\nu$, with strain is proportional to the fibre modulus then we can write

$$\frac{d\Delta\nu}{d\varepsilon} \propto E = \frac{d\sigma}{d\varepsilon} \qquad (1)$$

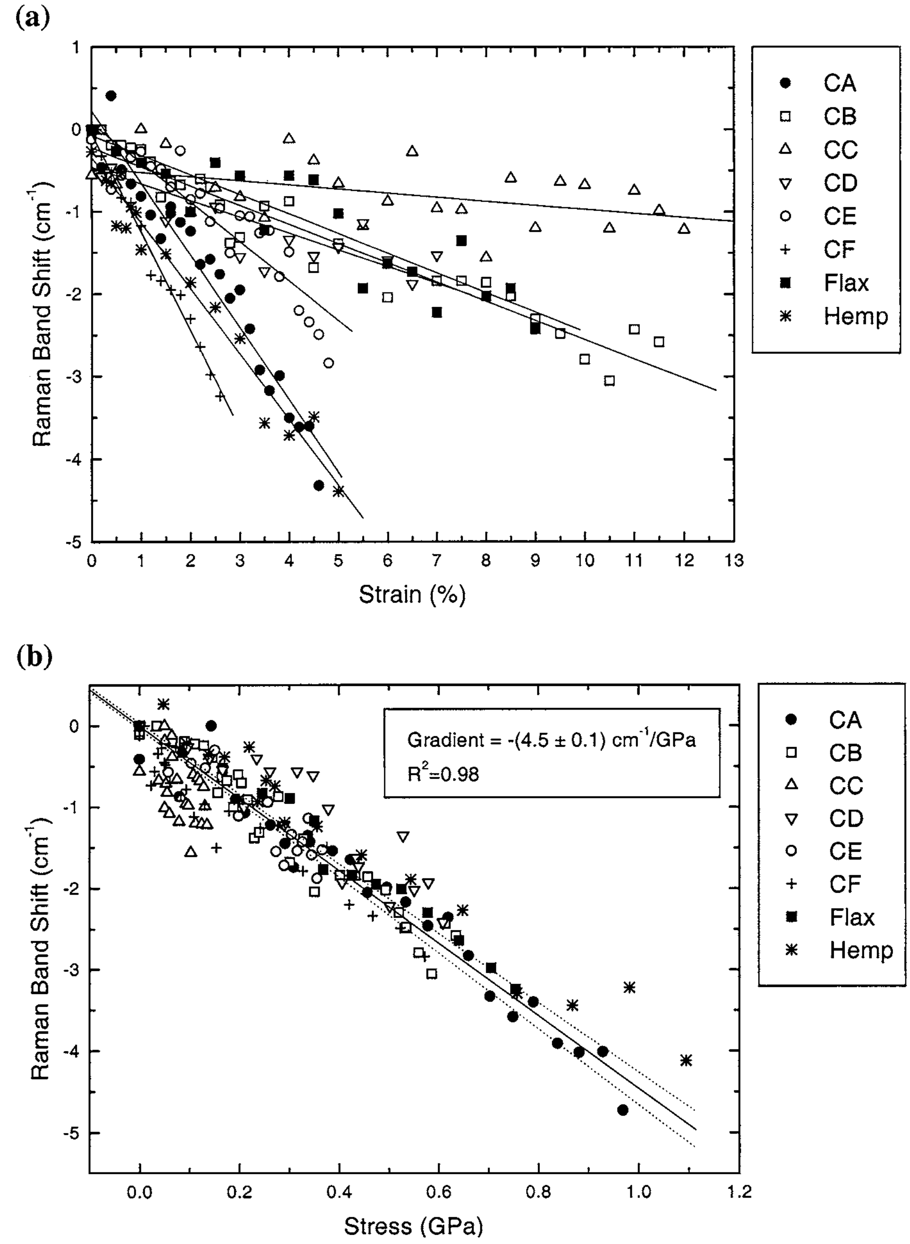

Figure 5 (a) Strain and (b) stress dependent Raman band shifts of the 1095 cm^{-1} peak.

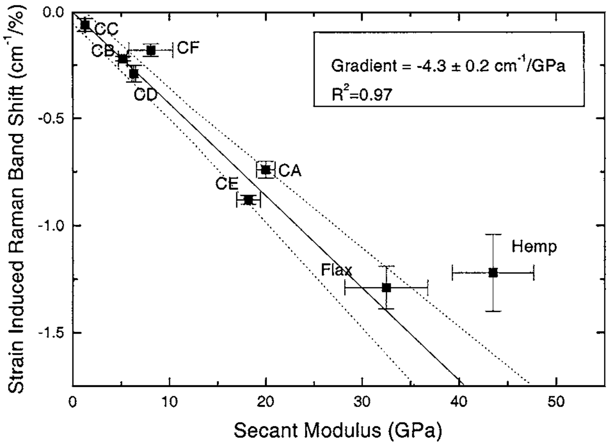

Figure 6 Relationship between the magnitude of the strain-induced Raman band shift rate and secant modulus of cellulose fibres (Dotted lines indicate the upper and lower 95% confidence bands.

which confirms that the shift of band position should be proportional to stress (Fig. 5b).

3.2. Wood deformation

An example of a Raman spectrum for the wood is shown in Fig. 7. It was found that well-defined spectra could only be obtained for the wood samples when the laser beam was focused on a cell wall rather than on a facing plane as shown in the SEM micrograph, in Fig. 8. A stronger signal was also recorded with the laser beam polarised parallel to the cell wall and all measurements were undertaken using this configuration.

The 1095 cm^{-1} Raman peak in the wood samples also shifted towards a lower wavenumber during tensile deformation. The mean Raman shift for the wood samples (7 tested) is reported in Fig. 9 and it is immediately

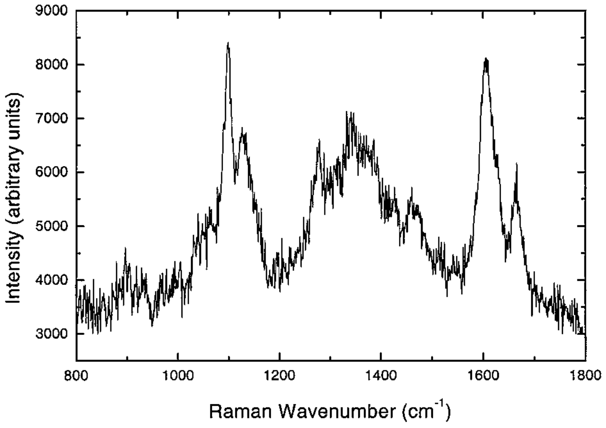

Figure 7 Raman spectrum of *Pinus radiata* wood.

obvious that there is variability. This is thought to be due to the fact that it is impossible to focus the laser spot onto one particular layer (S_1, S_2 or S_3). Since the layers differ in mechanical properties this variability could be quite marked. It is noted that the rates of band shift with strain for the flax and hemp fibres (-1.22 ± 0.18 and -1.29 ± 0.10 cm^{-1}/%) are of a similar order to the wood samples (-1.14 ± 0.34 cm^{-1}/%). This suggests from the relationship in Equation 1 that, at a given level of strain, the stress on the cellulose molecules is similar in the flax, hemp and wood materials.

No shift occurred for the 1600 cm^{-1} band (Fig. 7) corresponding to lignin [17] as has been reported elsewhere [18]. This does not mean that the lignin is not deformed. Lignin is a low modulus amorphous polymer [19] that acts as the matrix material in the wood "composite" structure [20], and it is possible that no shift is seen in its characteristic peak because it is non-load bearing.

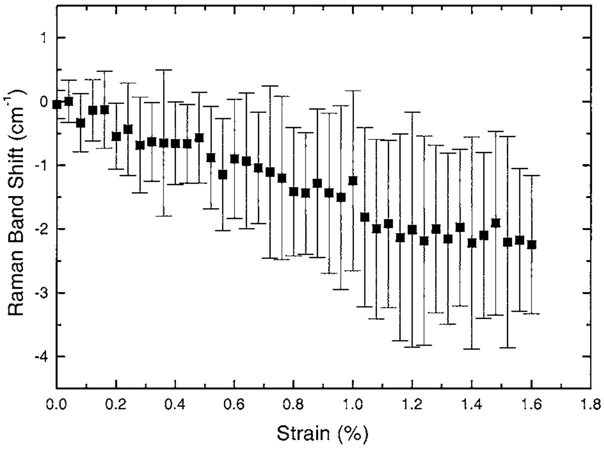

Figure 9 The variation of Raman band shift with tensile strain obtained using the four-point bending test for 7 different pine wood samples.

3.3. Paper deformation

The Raman spectrum for the cotton paper is shown in Fig. 10a and it can be seen that it is similar to that obtained for the natural cellulose fibre shown in Fig. 3. Stress induced Raman shifts were also observed with the paper samples. It was noted that fibres with a flatter and wider cross section gave the best spectra. Also clearer Raman shifts, an example of which is reported in Fig. 10b, were obtained for fibres of this type. This is thought to be due to the fact that greater surface area is available for inter-fibre bonding with these fibres, and strain applied to the sheet is more likely to be transferred to these fibres.

The deformation of the paper samples, as reported in Fig. 10b can be separated into three distinct phases. Initially Raman band position of the fibre being monitored within the sheet shifts approximately

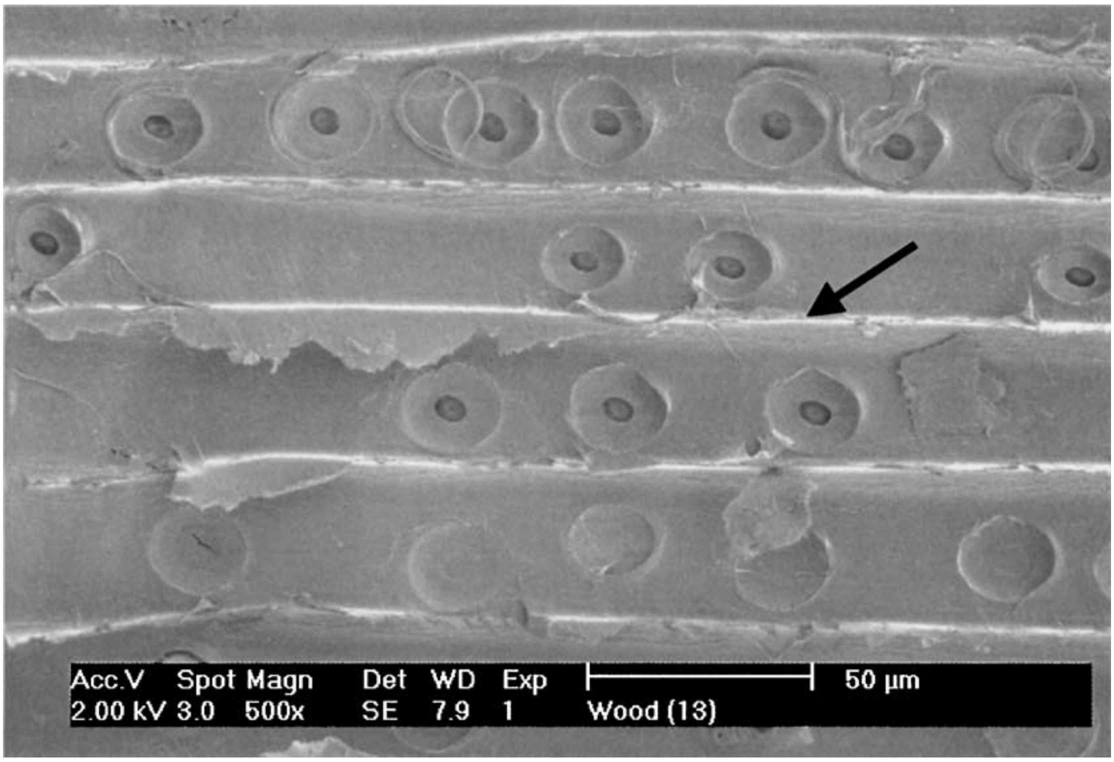

Figure 8 An SEM micrograph of a specimen of wood showing the region in which the laser was focussed (arrow).

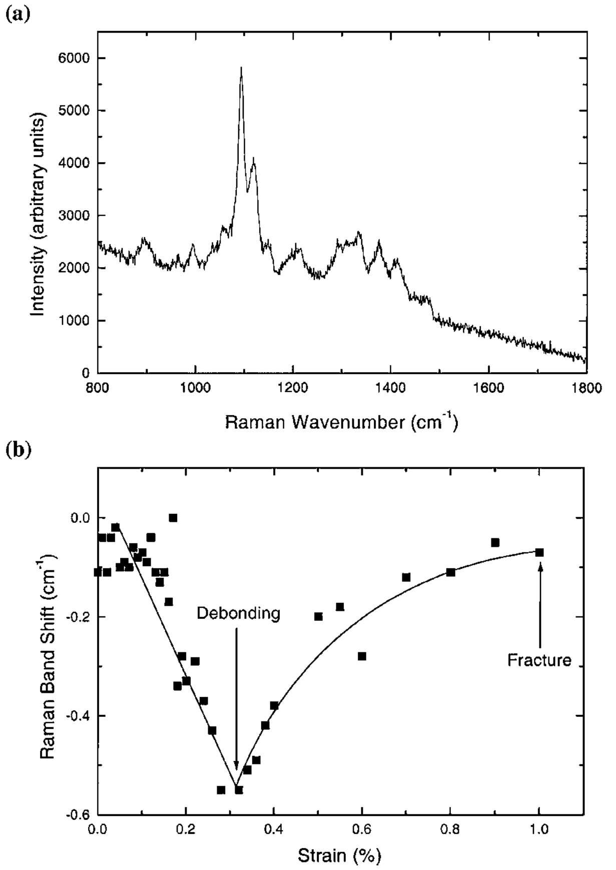

Figure 10 Examples of (a) a Raman spectrum of cotton paper at zero strain and (b) the shift of the 1095 cm^{-1} Raman band with tensile strain for cotton paper.

linearly with strain, as with the single regenerated and natural cellulose fibres, with a strain sensitivity of (-1.46 ± 0.22) cm^{-1}/%. This corresponds to elastic deformation of the fibre within the paper network. After this region there is an inflexion point where the fibre appears to debond from the network. Non-linear relaxation of the stress on the fibre then occurs, with almost full recovery, up to the point where the paper fractures. This corresponds to slippage of the fibre within the network leading to eventual failure. This is a clear demonstration of how the Raman technique can be used to monitor the local deformation micromechanics of fibrous networks.

4. Conclusions

Raman spectroscopy is a powerful technique that can be applied to study the deformation of a wide variety of polymeric materials, and it has been shown from this work that it is particularly useful for a number of cellulosic materials. The shifts of the 1095 cm^{-1} band in the cellulose spectrum gives information on the direct molecular deformation of the material, and this work has shown that this effect is indicative of the stress in the fibres. The invariance of the shift rate with stress, no matter what supposed cellulose crystal structure or specific mechanical property of the fibre confirms their structures could be modelled using a modified series aggregate model, as reported previously [1, 5]. This technique has also been shown to be a useful tool in analysing composite systems; namely paper and wood. In particular it is found that the wood samples behave like typical unidirectional composites, with the lignin matrix bearing little load and the cellulose acting as the reinforcement. In paper the deformation of single fibres within the sheet can be followed and the processes of fibre deformation and slippage identified.

Acknowledgements

This work was completed using funding via EPSRC grant No. GR/M82219 and from the Thai government (JS). The authors would also like to thank Dr. Bill Sampson, Department of Paper Science, UMIST for helpful discussions and the paper samples, Dr. Maurits Northolt of ACORDIS for supplying regenerated cellulose fibres (CA-CE) and to Emeritus Prof. K. M. Entwistle for the wood samples.

References

1. W.-Y. YEH and R. J. YOUNG, *Polymer* **40** (1999) 85.
2. C. WOODCOCK and A. SARKO, *Macromolecules* **13** (1980) 1183.
3. A. SARKO and R. MUGGLI, *ibid.* **7** (1974) 480.
4. S. J. EICHHORN, M. L. HUGHES, R. SNELL and L. MOTT, *J. Mater. Sci. Lett.* **19** (2000) 721.
5. S. J. EICHHORN, R. J. YOUNG and W.-Y. YEH, *Textile Research Journal* **71**(2) (2001) 121.
6. A. J. PANSHIN and DE C. ZEEUW, in "Textbook of Wood Technology" (McGraw-Hill, New York, 1970).
7. L. MOTT, S. M. SHALER and L. H. GROOM, *Wood and Fiber Science* **28** (1996) 429.
8. P. NAVI, P. K. RASTOGI, V. GRESSE and A. TOLOU, *Wood Science and Technology* **29** (1995) 411.
9. H. L COX, *Brit. J. Appl. Phys. 3* (1952) 72.
10. D. H. PAGE, *Tappi J.* **52**(4) (1969) 674.
11. O. KALLMES, G. BERNIER and M. A. PEREZ, *Paper Tech. and Ind.* **18** (1977) 222, 243, 283, 328.
12. K. M. ENTWISTLE and N. J. TERRILL, *J. Mater. Sci.* **35** (2000) 1675.
13. D. W. MARQUARDT, *J. Soc. Ind. Appl. Math.* **11** (1963) 431.
14. R. H. ATALLA and S. C. NAGEL, *Science* **185** (1974) 522.
15. R. H. ATALLA, *Appl. Polym. Symp.* **28** (1976) 659.
16. R. J. YOUNG, *J. Text. Inst.* **86** (1995) 360.
17. R. H. ATALLA and U. P. AGARWAL, *Science* **227** (1985) 636.
18. J. SIRICHAISIT. Ph.D. Thesis, UMIST, UK, 2000.
19. W. G. GLASSER, in "Pulp and Paper Chemistry and Chemical Technology" (Wiley InterScience, New York, 1980) p. 39.
20. D. HULL and T.W. CLYNE, "An Introduction to Composite Materials," 2nd ed., (Cambridge University Press, 1996).

Received 25 September
and accepted 23 November 2000